28

ASSESSMENT OF SATELLITE RAIN RETRIEVAL ERROR PROPAGATION IN THE PREDICTION OF LAND SURFACE HYDROLOGIC VARIABLES

Emmanouil N. Anagnostou
Civil and Environmental Engineering, University of Connecticut, Storrs, CT, USA

1 INTRODUCTION

Precipitation is probably the most important component of a mixture of hydrologic cycle parameters (precipitation, soil moisture, evapotranspiration, runoff, etc.), mostly accountable for shaping the climatic state of water in the earth stores, its variability, and climatic trends. Understanding the interactions and feedback between precipitation and land surface processes is key to advancing the predictability of the water cycle at scales varying from mesoscale to regional and climate. Unfortunately, precipitation simulated by global climate models is not sufficiently accurate for directly forcing surface energy and water budgets in coupled land–atmosphere data assimilation systems. This uncertainty has an effect on the study of interactions between land surface process and atmospheric convection. A perceived solution is the use of radiation budget and precipitation estimates from ground and/or space-based sensors to force off-line land data assimilation systems (LDAS). In a recent report, Mitchell et al. (1999) emphasized on the viability of the land surface alternative to coupled systems. This approach uses uncoupled physically based LDAS systems (Koster and Suarez 1996; Liang et al. 1996; Mitchell et al. 2000) driven by surface forcing anchored by independent observation-based precipitation and radiation budget fields.

A critical aspect associated with such an approach is the need to resolve the precipitation variability over large regions with high temporal (of the order of 1–3 h) and spatial (0.05° × 0.25°) resolution. Precipitation estimates over large regions (in particular over the tropical convective zones) are primarily

V. Levizzani et al. (eds.), Measuring Precipitation from Space: EURAINSAT and the Future, 357–368.
© 2007 *Springer.*

available from microwave (MW) and infrared (IR) sensor observations onboard earth-orbiting and geostationary satellite platforms, respectively. Overland MW channels measure the emission and scattering by precipitating ice and hydrometers, which is physically related to the water content, and indirectly to surface rainfall rate. The IR channel measures the thermal radiation emitted by clouds (or the surface) that is related to the temperature of the emitting media (cloud tops). As a consequence, cold clouds are assumed to have large vertical extent and be associated with precipitation beneath. Although, MW channels are associated with more definitive precipitation estimates than IR, observations from earth-orbiting satellites carrying MW sensors offer intermittent coverage (currently this is about six observations per day counting all available satellite platforms). Consequently, there has been significant effort to bridge those gaps estimating precipitation from proxy parameters inferred from the half-hourly geostationary IR observations (e.g., Anagnostou et al. 1999; Adler et al. 2000).

Improvement of geosynchronous satellite precipitation retrievals through regional calibration by the use of MW rain estimates, and by combining estimates from multiple sensors is currently approached in a number of studies (Hsu et al. 1999; Todd et al. 2001; Huffman et al. 2003). A common observation from these studies is that MW-calibrated IR-based rain retrievals are limited in terms of their ability to sufficiently characterize the surface rainfall variability. This is due to the weak physical relationship of IR measurement to convective rain processes. For example, Todd et al. (2001) showed 0.3 correlations and 350% standard error at high spatial (0.1 degree) and temporal (hourly) resolution in comparison with radar data. At coarser scale (1-degree daily) the same data comparison demonstrated a reduction of standard error to 90%.

To improve upon this limitation recent studies have combined hourly IR rain retrievals with the infrequent passive MW estimates using data fusion approaches (see papers in Section 4 of this book). It is not well understood, though, how to optimally combine rain products of different resolutions, sampling frequencies, and retrieval error characteristics. For example, which is better representative for a 3-hourly/0.5-degree grid rain estimate: an infrequent MW retrieval that is closer related to precipitation or a 6-hourly rain average from frequent IR observations but indirectly related to rainfall? A merging of estimates that is followed by spatial and temporal aggregation would most likely correspond to the best estimate. Given, though, the large influence that sampling and retrieval error characteristics have on the merged product, a definitive answer about data fusion cannot be obtained without proper error investigation studies.

The impact of satellite rain estimation error on the simulation of hydrological variables (else known as error propagation) has not been well investigated. Hossain and Anagnostou (2004) and Hossain et al. (2004)

recently studied the adequacy of current satellite rain retrievals in terms of flood prediction for medium-sized watersheds. An earlier study by Nijssen and Lettenmaier (2003) examined the effect of precipitation error due to satellite sampling alone on the simulation of runoff and other hydrological variables derived from a macroscale hydrological model. Although, these studies offered valuable information on the hydrological error characteristics of satellite retrievals they are based on stochastic error models with limited representation of the true estimation error characteristics. There is a clear need to further our understanding on this issue on the basis of experimental investigations that would use actual satellite rain retrieval data and hydrologic models.

In this paper, we present such an experimental framework aimed at evaluating hydrologic relevant rain retrieval merging techniques. The framework includes a physically based land surface model (LSM) implemented in a data-rich region, and uses satellite rain retrievals from MW and IR observations. The selected region for this experiment is an area covered by the Oklahoma hydrometeorological station network (MESONET). The area is under the coverage of the National Weather Service Weather Surveillance Radar (WSR-88D) network, and of an array of MW satellites (TRMM, SSM/I). The community land surface model (CLSM) (Bonan et al. 2002) was used in this study. It was forced by radiation and meteorological (winds, temperature, and relative humidity) field data measured by the Oklahoma MESONET. High-resolution (hourly at 4×4 km^2) rain gauge-calibrated radar (WSR-88D) rainfall fields were used as ground reference of precipitation (Fulton et al. 1998). This experimental framework was the basis for assessing two satellite rain retrieval schemes and evaluating their error structure in the prediction of hydrological and other land surface parameters. We will argue that limiting the evaluation of rain retrievals at the level of rain rate estimation error is not sufficient to identify retrieval techniques that are optimal in terms of other hydrological variables (e.g., runoff, soil moisture). The propagation of rain estimation error characteristics to the various hydrologic variables is complex and highly nonlinear, which calls for integrated error studies in rain estimation land surface modeling.

In the subsequent sections we present a short description of CLM followed by the study area and data. We will then describe the satellite rain retrievals and present the simulation experiment where we evaluated the error statistics in the estimated rainfall and land surface hydrological variables. We close with a summary of our findings, and suggestions on the research direction for developing hydrologic relevant satellite rain retrievals.

2 THE LAND SURFACE MODEL

The CLM is devised in this study to simulate land surface parameters. It is a column (one-dimensional [1D]) model developed on the basis of the Bonan (1996) LSM, which was modified to incorporate the best features of the Dickson et al. (1986) Biosphere–Atmosphere Transfer scheme and the Dai et al. (1997) IAP94 LSM. CLM has one vegetation layer as in most LSMs, ten unevenly spaced vertical soil layers with variable hydraulic conductivity, and up to five snow layers depending on the total snow depth. The surface grid cell can be subdivided into a number of tiles that consist of a single type of land cover. The model performs the water and energy balance calculations over each tile at every time step. Most surface processes such as evaporation from the ground, transpiration from the plants root zone, soil and snow water propagation, leaf temperature and fluxes, soil and snow temperature, and phase change are parameterized through physical–empirical equations. Nevertheless, the parameterization of runoff-related processes in soil–vegetation–atmosphere interaction is not well formulated, which is perhaps one of the weak points of CLM. The runoff parameterization is based on TOPMODEL (Beven and Kirkby 1979) concept, while river routing model is not included. With externally forcing data (precipitation, radiation, wind speed, air temperature, and humidity) CLM computes a number of prognostic variables that include runoff, soil moisture, temperature in the soil layer, water intercepted on the canopy, leaf temperature, latent heat flux, and sensible heat flux.

3 STUDY AREA AND DATA

The study region covers two 1-degree grid areas in Oklahoma associated with distinct vegetation cover. The center of the lowly vegetated 1-degree site (hereafter named L_{veg}) is at 34.6861N latitude and –99.8339W longitude; and it includes five MESONET stations. The dominant vegetation type is non-arctic grass (type 13 in CLM), while the soil sand and clay percentages are 47% and 19%, respectively. The average value of leaf area index (LAI) for this site in June is 1.3. The center of the highly vegetated 1-degree site (hereafter named H_{veg}) is 35.4360N latitude and –94.7740W longitude; it also includes five MESONET stations. The dominant vegetation type for H_{veg} is broadleaf deciduous temperate tree (type 7 in CLM), while the soil sand and clay percentages are 54% and 23%, respectively. The average value of LAI for this site in June is 5.3.

Two types of data are needed to run CLM: land surface data, and hydrometeorological forcing data. The land surface data that include vegetation cover type, vegetation fraction, monthly leaf and stem area index, canopy top and bottom heights, and soil texture and color are available in CLM global

database and considered along with the model parameterizations as true representations of the land surface processes. Those data are available at 1-km spatial resolution and were mostly derived from space-borne remote-sensing observations such as the IGBP DISCover data set (Loveland et al. 2000), University of Maryland tree cover data set (DeFries et al. 2000a,b), advanced Very High Resolution Radiometer (AVHRR), and the IGBP soil data set (Global soil Data task, 2000). The hydrometeorological data include grid-averaged values of (1) meteorological measurements from the MESONET stations (Brock et al. 1995); and (2) rainfall rates from WSR-88D. The radar rainfall fields are extracted from the National Radar Rainfall Mosaic available at the Hydrologic Rainfall Analysis Product (HRAP) ~4-km resolution (Fulton et al. 1998). These estimates have been corrected for a number of radar error sources including mean field bias based on a scheme that uses hourly area-averaged rain gauge-to-radar rainfall ratios (Seo et al. 1999, 2000). The WSR-88D rain estimates are used here as the reference ground rainfall data set, against which we will assess the rainfall fields derived from the satellite retrievals. The experimental data span a period from 1 January to 30 September 2002.

4 SATELLITE RAINFALL ESTIMATES

Two satellite rain retrieval schemes are evaluated in this study. The first is based on MW-calibrated IR rain estimates, while the second on a merging of those estimates with instantaneous precipitation fields derived from TRMM Microwave Imager and three Special Sensor Microwave/Imager (F13, F14, and F-15) passive MW observations on the basis of Grecu and Anagnostou (2001) overland algorithm. The IR rain retrieval is part of a variable rainfall product (VAR) array produced in real time at NASA Goddard Space Flight Center by Huffman et al. (2003), and is referred to as 3B41RT product (ftp://aeolus.nascom.nasa.gov). The VAR retrieval incorporates the NOAA Climate Prediction Center half-hourly Global IR composites (Janowiak et al. 2000) aggregated to 0.25-degree spatial grid resolution and hourly accumulations. The technique uses coincidental IR observations with MW rain retrievals from TMI and SSM/I observations to dynamically (on a month-to-month basis) calibrate the IR rain algorithm at discrete 5-degree grid areas. The calibration is based on matching the probability density histograms of IR brightness temperatures and MW rain rates falling within a common data set.

The second technique is a merging MW/IR scheme. The scheme identifies for every hourly IR rainfall value at 0.25-degree pixel resolution all available instantaneous MW estimates that are within a ±6 h time window. The following approach is then used to merge the MW and IR rain values for any given pixel:

- If MW > 0 and IR > 0: the merged value is based on an error variance-weighted averaging.
- If MW = 0 and IR = 0: the merged value is zero.
- If MW > 0 and IR = 0 or MW = 0 and IR > 0: the rain/no-rain decision is made according to the sensor with the highest rain detection Heidke skill score (HSS) (Heidke 1926).

The error variance and HSS statistics for MW and IR rain retrievals were evaluated using as reference matched hourly WSR-88D rainfall fields. Table 1 shows those statistics. Note a deviation in the rainfall error statistics between the SSM/I and TMI MW sensors. The MW error statistics were augmented by a representativeness error term used to account for the large time lags between a MW overpass and a certain hourly rain estimate. For this purpose we used hourly radar rainfall fields to determine the error variance and rain detection HSS score as function of time lag. The error statistics are shown in Fig. 1.

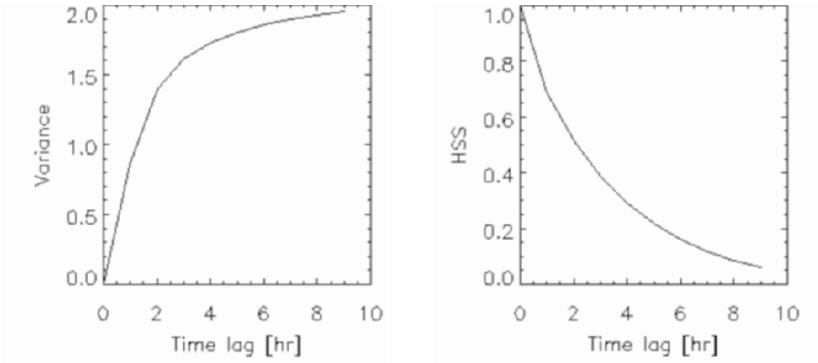

Figure 1. Representativeness error variance (*left*) and HSS score (*right*) presented as function of time lag.

Table 1. Error variance and HSS of MW and IR rainfall estimates.

	MW (TMI)	MW (SSM/I)	IR
Variance	0.65	0.8	1.65
HSS	0.41	0.37	0.1

5 SIMULATION EXPERIMENT AND RESULTS

As mentioned in the Introduction, this study aims at studying the effect of rainfall retrieval error on the simulation of land surface parameters assuming

that our knowledge of the physical processes and other input parameters is accurate. The CLM, which provides a physically based framework for land surface processes, is used to model the 1D grid-averaged processes at two distinct, in terms of vegetation cover, sites. Three simulation scenarios are considered where CLM is forced with the three different rainfall data sets (radar, IR, and merged MW/IR). During the spin-up period of the model (January to April) the grid-averaged radar rainfall was commonly used as input to the model. The other meteorological forcing parameters such as radiation budget, air temperature, wind speed, and relative humidity were based on grid-averaged MESONET measurements, which were considered to be associated with insignificant error. Consequently, the only source that would differentiate the predicted land surface variables among the three simulation scenarios is the differing precipitation input. This difference is defined in relative terms as following:

$$\varepsilon_x = \frac{V_x - V_{\text{ref}}}{V_{\text{ref}}} \tag{1}$$

V is used to symbolize the different hydrologic variables (including precipitation). Subscript "x" refers to the variables predicted from satellite IR or merged rain estimates and subscript "ref" refers to variables predicted on the basis of grid-averaged rain gauge-calibrated radar rainfall. The land surface variables evaluated in this study are: latent heat flux (LE), sensible heat flux (SH), surface runoff (R_{off}), soil moisture content at 21 cm depth (θ_S), and soil temperature at 21 cm depth (θ_T).

In Table 2 we summarize the relative error (ε) statistics (mean and standard deviation [STD]) of the two satellite retrievals in terms of precipitation and CLM-predicted variables. The statistics are presented for three spatial scales (0.25, 0.5, and 1 degree) and the two vegetation regimes (H_{veg} and L_{veg}). A first general observation is that the merged rain retrieval is associated with less bias and error variance in all predicted variables compared to the IR rain retrieval. In terms of bias (or mean error) we note an almost 250% increase between low (L_{veg}) and high (H_{veg}) vegetation sites for the IR retrieval, while the corresponding increase in the case of merged rain estimates is moderate (~80%). An interesting observation for the IR retrieval is that the rain estimation bias magnifies significantly in runoff prediction (~3 times) in the case of L_{veg}, while the corresponding runoff-to-rainfall bias ratio for the merged rain retrieval is almost one. In the case of H_{veg} site the runoff bias

Table 2. Error statistics (bias and STD) of rainfall and CLM-predicted variables derived from the simulation experiment.

		Mean error (bias)			STD		
		0.25°	0.5°	1.0°	0.25°	0.5°	1.0°
L_{veg}	P	60 (26)	60 (26)	60 (26)	124 (113)	129 (113)	130 (109)
	LE	34 (19)	31 (18)	32 (18)	76 (69)	74 (67)	68 (60)
	SH	–26 (–15)	–25 (–14)	–27 (–16)	35 (30)	34 (30)	32 (27)
	R_{off}	115 (37)	115 (35)	116 (30)	187 (144)	213 (148)	232 (146)
	θ_S (21 cm)	7 (0.5)	7 (0.2)	8 (0.2)	113 (117)	108 (110)	118 (120)
	θ_T (21 cm)	–0.5(–0.3)	–0.4(–0.2)	–0.4(–0.2)	40 (34)	39 (32)	36 (29)
H_{veg}	P	–12 (–15)	–12 (–15)	–12 (–15)	93 (88)	88 (81)	76 (67)
	LE	–11 (–6)	–12 (–7)	–14 (–8)	49 (44)	49 (44)	47 (42)
	SH	13 (7)	15 (9)	17 (10)	29 (26)	29 (26)	27 (24)
	R_{off}	–7 (–24)	–7 (–25)	–6 (–27)	93 (79)	91 (71)	92 (59)
	θ_S (21 cm)	–5 (–4)	–5 (–4)	–5 (–3)	71 (52)	63 (43)	60 (41)
	θ_T (21 cm)	0.02 (0.0)	0.02 (0.0)	0.05 (0.0)	15 (13)	15 (13)	13 (10)

seems to reduce (smoothing effect) by about 30%. In terms of soil moisture and other variables, we note a significant reduction of bias for both satellite retrievals and vegetation sites.

In terms of the relative STD error statistic our observations are the following. We demonstrate a moderate reduction of STD from L_{veg} to H_{veg}, and notable spatial scale dependence for STD in the H_{veg} regime. The STD of rainfall, runoff, and soil moisture error for the merged (IR) rain estimates reduces by an average of 23% (12%) going from 0.25 to 1-degree grid resolution. We show magnification in the error STD going from rainfall to runoff variable, and a smoothing effect for all other variables. The rate of STD magnification for the IR retrieval exhibits a spatial scale dependence (ranging from 60% to 80%) in the case of L_{veg}, while the corresponding rate of magnification for the merged rain estimate is consistent across the scales at ~30%. In H_{veg} site the IR retrieval error STD magnification in runoff is shown to vary from about 5% (at 0.25 degree) to 25% (at 1 degree), while for the merged rain estimates we note a consistent smoothing effect (~10% error reduction). In all other variables the STD error propagation is associated with smoothing, which varies across the different variables. In soil moisture, for example, the STD reduces by about 12% (8%) in the merged (IR) retrieval case. The error STD smoothing is significant for the energy-related variables and fluxes

(θ_T, LE, and LH), indicating that errors in precipitation alone would have minimal effect in those variables.

We finally used our experimental data to investigate the spatial structure of error in the various hydrological and land surface variables. This is presented in Fig. 2 in terms of spatial correlation of error (ε) as function of distance. We present two curves in each panel, one representing the IR and the second the merged rain retrievals. Left and right panels represent L_{veg} and H_{veg} sites, respectively. We make the following observations. First, error in rainfall and runoff decorrelate faster than in the other variables. Second, the IR retrieval error is associated always with lower lag-correlation than the corresponding IR retrieval error. This explains why spatial averaging resulted in a more significant STD reduction in the merged case compared to the IR retrieval case.

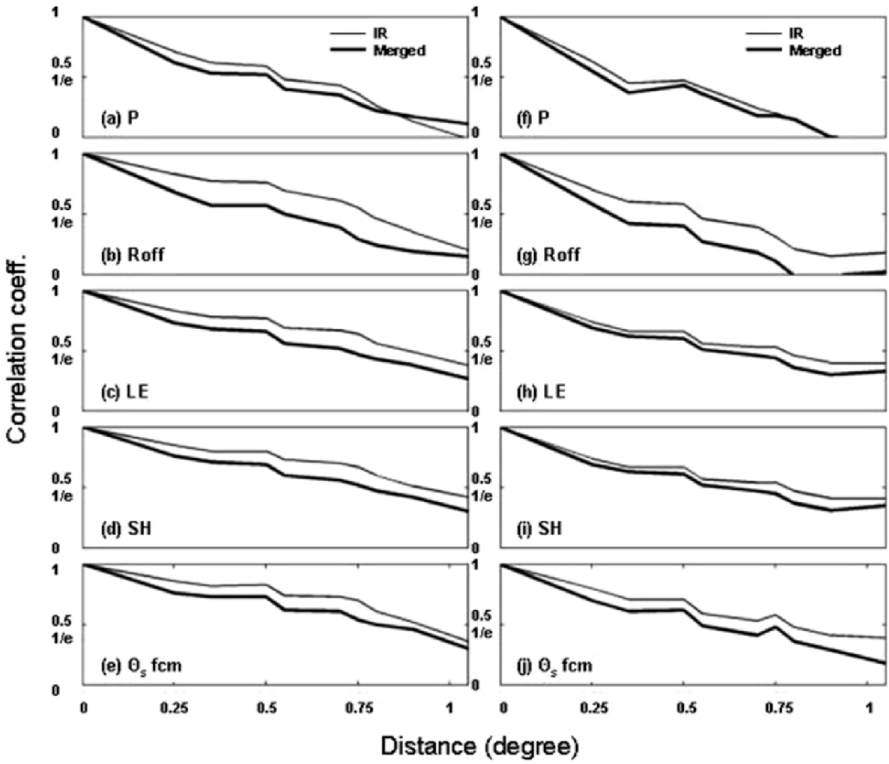

Figure 2. Spatial lag-correlation of error. Left and right panels correspond to L_{veg} and H_{veg} sites, respectively.

6 CLOSING REMARKS

This paper presented a framework for investigating hydrologically relevant satellite rain retrievals. The strategy adopted is, firstly, to compile the hydrometeorological variables needed by an LSM including three different sources of precipitation data, i.e., gauge-calibrated radar rainfall and two satellite retrieval (an IR and a merged MW/IR rain retrieval), assuming that the model parameters are well representative of the land surface processes. The CLM was selected to simulate the land surface processes at three scales, 0.25, 0.5, and 1 degree, and two distinct vegetation conditions. Simulated results from the two satellite rain retrieval-forcing parameters were compared to corresponding simulations derived from the radar rainfall input considered as reference. The primary conclusions of the present study are as follows:

- Rainfall error propagates nonlinearly in hydrologic simulation uncertainty-precipitation error structure and land surface conditions affect this error propagation (we noted this specifically in the case of runoff, and to a lesser extent in soil moisture).
- Error variance reduces (nonlinear smoothing effect) in most of the hydrological variables and fluxes, but runoff.
- We noted lower error statistics when using the merged MW/IR rain input compared to the IR-only input.
- Overall, spatial averaging reduces the error in most of the land surface variables, but this reduction depends on the rain retrieval error characteristics and land surface conditions.

An important observation from this study is that the effect of vegetation and structural characteristics of rain retrieval error are factors affecting the error propagation in land surface variables. This study investigated only a limited number of land surface conditions and satellite retrieval schemes and, thus, should only be viewed in a qualitative sense. Apparently, using different rain retrievals and hydrometeorological regimes could lead to different error characteristics. We would like to view this experimental error propagation framework as the basis for achieving a more comprehensive hydrologic assessment of satellite retrievals, and/or for developing merging techniques that would optimize hydrological prediction error statistics.

7 REFERENCES

Adler, R. F., G. J. Huffman, D. T. Bolvin, S. Curtis, and E. J. Nelkin, 2000: Tropical rainfall distributions determined using TRMM combined with other satellite and rain gauge information. *J. Appl. Meteor.*, **39**, 2007–2023.

Anagnostou, E. N., A. J. Negri, and R. F. Adler, 1999: A satellite infrared technique for diurnal rainfall variability studies. *J. Geophys. Res.*, **104** (D24), 31477–31488.

Beven, K. J. and M. J. Kirkby, 1979: A physically based variable contributing area model of basin hydrology. *Hydrol. Sci. Bull.*, **24**, 43–69.

Bonan, G. B., 1996: A land surface model (LSM version 1.0) for ecological, hydrological, and atmospheric studies: Technical description and user's guide. *NCAR Technical Note*, NCAR/TN-417+STR, Boulder, CO.

Bonan, G. B., S. Levis, L. Kergoat, and K. W. Oleson, 2002: Landscapes as patches of plant functional types: an integrating concept for climate and ecosystem models. *Global change Biochem Cycles*, **16** (2), Art No. 1021.

Bonan, G. B., K. W. Olsen, M. Vertenstein, S. Levis, X. B. Zeng, Y. J. Dai, R. E. Dickinson, and Z. L. Yang, 2002: The land surface climatology of the community land model coupled to the NCAR community climate model. *J. Climate*, **15**, 3123–3149.

Brock, F. V., K. C. Crawford, R. L. Elliot, G. W. Cuperus, S. J. Stadler, H. L. Johnson, and M. D. Eilts, 1995: The Oklahoma Mesonet: a technical overview. *J. Atmos. Oceanic Technol.*, **12**, No. 1, 5–19.

Dai, Y. J. and Q. C. Zeng, 1997: A land surface model (IAP94) for climate studies 1: formulation and validation in off-line experiments. *Adv. Atmos. Sci.*, **14**, 433–460.

DeFries, R. S., M. C. Hansen, and J. R. G. Townshend, 2000a: Continuous fields of vegetation characteristics: a linear mixture model applied to multi-year 8 km AVHRR data. *Int. J. Remote Sens.*, **21**, 1389–1414.

DeFries, R. S., M. C. Hansen, J. R. G. Townshend, A. C. Janetos, and T. R. Loveland, 2000b: A new global 1-km dataset of percentage tree cover derived from remote sensing. *Global Change Biol.*, **6**, 247–254.

Dickson, R. E., A. Henderson-Sellers, P. J. Kennedy, and M. F. Wilson, 1986: Biosphere-Atmosphere Transfer Scheme (BATS) for the NCAR community climate model. Technical Note; NCAR/TN-275+STR, NCAR, Boulder, CO.

Fulton, R. A., J. P. Breidenbach, D. J. Seo, D. A. Miller, and T. O'Bannon, 1998: The WSR-88D rainfall algorithm. *Wea. Forecasting*, **13** (2), 377–395.

Global Soil data Task, 2000: Global soil data products CD-ROM (IGBP-DIS). International Geosphere-biosphere Programme – data and Information Available Services. Available at: http://www.daac.ornl.gov

Grecu, M. and E. N. Anagnostou, 2001: Overland precipitation estimation from TRMM passive microwave observations. *J. Appl. Meteor.*, **40** (8), 1367–1380.

Hossain, F., E. N. Anagnostou, and T. Dinku, 2004: Sensitivity analyses of satellite rainfall retrieval and sampling error on flood prediction uncertainty. *IEEE Trans. Geosci. Remote Sens.*, **42**, 130–139.

Hsu, K., X. Gao, S. Sorooshian, and H. V. Gupta, 1997: Precipitation estimation from remotely sensed information using artificial neural networks. *J. Appl. Meteor.*, **36** (9), 1176–1190.

Huffman, G. J., R. F. Adler, E. F. Stocker, D. T. Bolvin, and E. J. Nelkin, 2003: Analysis of TRMM 3-hourly multi-satellite precipitation estimates computed in both real and post-real time. *Proc. 12th Conf. Sat. Meteor. and Oceanog.*, 9–13 Feb. 2003, Long Beach, CA.

Huffman, G. J, R. F. Adler, M. M. Morrisey, D. T. Bolvin, S. Curtis, R. Joyce, B. McGavock, and J. Susskind, 2001: Global precipitation at one degree daily resolution from multisatellite observations. *J. Hydrometeor.*, **2**, 36–60.

Janowiak, J. E., R. J. Joyce, and Y. Yarosh, 2000: A real-time global half-hourly pixel resolution infrared dataset and its applications. *Bull. Amer. Meteor. Soc.*, **82**, 205–217.

Koster, R. and M. Suarez, 1996: Energy and water balance calculations in the MOSAIC LSM. *NASA Tech Memo 104606*, Vol. 9.

Liang, X., E. Wood, and D. Lettenmaier, 1996: Surface and soil moisture parameterization of the VIC-2L model: Evaluation and modifications. *Global Planet. Change*, **13**, 195–206.

Loveland, T. R., B. C. Reed, J. F. Brown, D. O. Ohlen, Z. Zhu, L. Yang, and J. W. Merchant, 2000: Development of a global land cover characteristics database and IGBP DISCover from 1 km AVHRR data. *Int. J. Remote Sens.*, **2**, 1303–1330.

Mitchell, K. and Co-authors, 1999: GCIP Land Data Assimilation System (LDAS) project now underway. *GEWEX News*, **9** (4), 3–6.

Mitchell, K. and Co-authors, 2000: Recent GCIP-sponsored advancements in coupled land-surface modeling and data assimilation in the NCEP Eta mesoscale model. *Prepr. 15th AMS Conf. on Hydrology*, Long Beach, CA, Paper P1.22.

Nijssen, B. and D. P. Lettenmaier, 2004: Effect of precipitation sampling error on simulated hydrological fluxes and states: Anticipating the Global Precipitation Measurement Satellites. *J. Geophys. Res.*, **109**, D02103, doi: 10.1029/2003JD003497.

Seo, D. J., J. Breidenbach, and R. Fulton, 2000: Real-time adjustment of range-dependent biases in WSR-88D rainfall estimates due to nonuniform vertical profile of reflectivity. *J Hydrometeor.*, **1** (3): 222–240.

Seo, D. J., J. P. Breidenbach, and E. R. Johnson, 1999: Real-time estimation of mean field bias in radar rainfall data. *J. Hydrology*, **223** (3–4): 131–147.

Todd, M. C., C. Kidd, D. Kniveton, and T. J. Bellerby, 2000: A combined satellite infrared and passive microwave technique for estimation of small scale rainfall. *J. Atmos. Oceanic Technol.*, **18**, 742–754.